Grzegorz Mazurek, Małgorzata Durlej, Marek Iwański
Structure and Environment 2021, vol. 13, (4), pp. 95-103, Article number: el 011
https://doi.org/10.30540/sae-2021-011

Structure and Environment
ISSN 2081-1500
e-ISSN 2657-6902
https://content.sciendo.com/sae
https://sae.tu.kielce.pl

sciendo

Kielce University of Technology

DOI: 10.30540/sae-2021-011

NUMERICAL MODELLING OF INTERLAYER ADHESION IN THE LAYER OF RECYCLED MATERIAL WITH THE USE OF THE LEUTNER APPARATUS AND COMPUTED TOMOGRAPHY SCANNING

NUMERYCZNE MODELOWANIE SCZEPNOŚCI MIĘDZYWARSTWOWEJ W WARSTWIE RECYKLOWANEJ Z WYKORZYSTANIEM BADAŃ W APARACIE LEUTNERA ORAZ TOMOGRAFII KOMPUTEROWEJ

Grzegorz Mazurek*, Małgorzata Durlej, Marek Iwański
Kielce University of Technology, Poland

Abstract

The work has investigated the actual mechanism of the adhesion between successive asphalt layers, taking into account the macrostructure of the pavement layers, which are made of heterogeneous materials. The interaction between the joined layers was determined by applying a cohesion contact model. The parameters of the model were identified using the results obtained in the course of the actual Leutner tests. The heterogeneity of the structure was mapped based on a digital image of a tomographic cross-section. The separation of the materials included in the individual layers was performed with the use of a script in the MatLab program. Thanks to this, the batch file for the Abaqus program was prepared thoroughly. As a result, it was possible to map as closely as possible the profile of the deformation caused by the loss of the interlayer adhesion. Based on the data analysis, it was found that in the layer of the base course constructed from cold-applied recycled materials, the loss of interlayer adhesion is related to the state of non-linear mastic deformation. As a consequence, it was found that large deformations in the mastic structure would cause losses of aggregate grains in the recycled layer. In addition, a large horizontal displacement within the layer of the base course made of recycled material is one of the likely causes of edge fractures in the road structure.

Keywords: inite element method, Leutner test, contact phenomena, calibration of the cohesion contact model

Streszczenie

W pracy został rozpoznany rzeczywisty mechanizm pracy połączenia między warstwami asfaltowymi uwzględniający makrostrukturę warstw nawierzchni, które są w istocie rzeczy materiałami niejednorodnymi. Interakcję pomiędzy łączonymi warstwami określono poprzez zastosowanie modelu kohezyjnego. Jego parametry zostały zidentyfikowane przy wykorzystaniu wyników pochodzących z rzeczywistych badań Leutnera. Niejednorodność struktury odwzorowano na podstawie cyfrowego obrazu przekroju tomograficznego. Separacja materiałów wchodzących w skład poszczególnych warstw została wykonana z wykorzystaniem skryptu w programie MatLab. Dzięki temu w sposób kompleksowy został przygotowany plik wsadowy do programu Abaqus. W rezultacie udało się odwzorować możliwie najwierniej stan odkształcenia, jaki powstaje w wyniku utraty sczepności międzywarstwowej. Na podstawie analizy danych stwierdzono, że w warstwie recy-

*Kielce University of Technology, Poland, e-mail: gmazurek@tu.kielce.pl

klowanej podbudowy w technologii na zimno utrata sczepności międzywarstwowej jest sprzężona z nieliniowym stanem odkształcenia w mastyksie. W konsekwencji stwierdzono, że duże odkształcenia w mastyksie spowodują w warstwie recyklowanej ubytki ziarn kruszywa. Ponadto duże przemieszczenia poziome w warstwie recyklowanej podbudowy są jedną z prawdopodobnych przyczyn odłamania krawędzi w konstrukcji drogi.

Słowa kluczowe: metoda elementów skończonych, badanie Leutnera, zjawiska kontaktowe, kalibracja modelu kohezyjnego

1. INTRODUCTION

In the design of new road pavement structures, aggregate-asphalt composites are treated as materials that match the elastic physical model [1]. It is a model that maintains a linear stress-strain relation [2]. Therefore, its use is limited to cases where the pavement structure is loaded for a short time of about 0.02 s at a temperature below +13°C. The key factor that affects the effectiveness of mapping the deformation state of the pavement structure layers is the proper determination of interlayer adhesion. The bonding layer is an indispensable element in the process of connecting two adjacent surfaces of the road construction layers and determines the effectiveness of the interlayer connection. In technological conditions, the bonding layer is made immediately before the application of the next layer of the pavement structure by sprinkling the already built-in layer with asphalt emulsion [3]. The loss of inter-layer adhesion causes an increase in deformation in successive layers of the pavement structure. As a result, each layer works separately, increasing the risk of exceeding the limit state due to high stress. In the pavement structure in which there has been a significant decrease in interlayer adhesion, the equivalent stiffness modulus of the entire pavement is reduced. As a result, the value of the vertical displacement (deflection) at the vehicle wheel interaction point is higher [4]. According to the studies carried out at the Gdańsk University of Technology, the loss of adhesion causing the increase in deflection may be caused by contamination of the contact surfaces, improper sprinkling, or a small amount of asphalt in the joined layers [3]. The increase in horizontal deformation is of particular importance in the case of the lower asphalt layers. 1% increase in horizontal deformation translates into a 3.9% service life decrease [5]. It should be noted that the deformation that may occur in the RCM-FB mastic phase may be much greater than deformation suggested by the study of sample deformation in the range of linear viscoelasticity [6, 7].

The performed tests and analyses aim to investigate the stress distribution in the contact zone between two structural layers with the use of the cohesion contact model. The cohesion contact model has been implemented into the numerical model. The heterogeneity of the layer structure was mapped using computed tomography scanning. The analysis of the stress distribution in the base course was also very important. The state of the interlayer connection was determined by using the Leutner apparatus test, which is the resultant of the effects that impact the quality of the connection.

2. MATERIALS AND METHODS

2.1. Pavement structure layer

2.1.1. The base course made of recycled material mixed with an innovative binder

As the base course, which is the object of the present analysis, a mix of recycled material, an innovative binder and foamed asphalt (RCM-FB) was used. The binder used in the mix had the following composition: 40% hydrated lime, 20% CEMI 32.5R cement and dust from a CBPD dedusting system [8]. Detailed research related to the optimisation of the binder composition can be found in the work [9, 10]. The granulation of the selected mix was coarse-grained (RCM-FB). The matrix of the recycled mineral mix was designed to have a high content of fine mineral particles. The presence of fine particles is important when using foamed asphalt since it ensures correct mastic production process parameters [11]. The particle size distribution curve is shown in Figure 1.

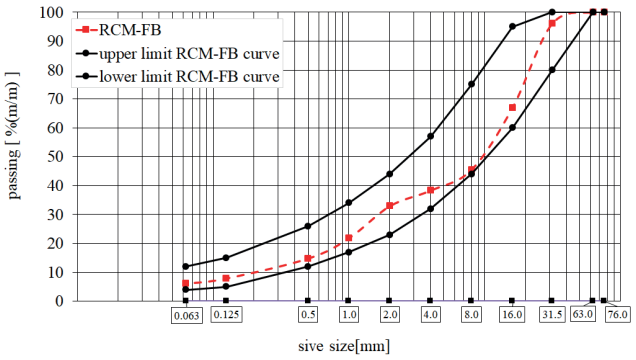

Fig. 1. RCM-FB granulation curve

The optimal content of the foaming water, which is 2.5% of the asphalt binders weight, was determined

using the results of the works [12, 11]. The amount of binder in the composition of the RCM-FB recycled mix was consistent with the amount assumed in the laboratory work, which is 3% (m/m).

2.1.2. Asphalt concrete layer

The asphalt concrete layer with the standard designation AC16W played the role of the binding layer (MMA). Its granulation has been selected by taking into account the effect of aggregate wedging. This is due to the conclusions contained in the work [13]. A significant impact of the granulation of the adjoining asphalt mixes on the interlayer adhesion was found. It is necessary to differentiate the grain size of the contacting layers and to limit the use of layers with the coarsest aggregate in the case of base courses and binding layers. The asphalt concrete layer created met the requirements of WT-2/2014 [14].

2.1.3. Leutner test

Cores with a diameter of 150 mm ±2 mm or 100 mm ±2 mm, drilled in the pavement or prepared according to the laboratory instructions, were used as samples. Samples prepared in the laboratory are compacted according to PN EN12697-31 or PN EN12697-33. Two cores drilled on one site but in remote from one another location should be used for the test. A diagram of the Leutner apparatus is shown in Figure 2.

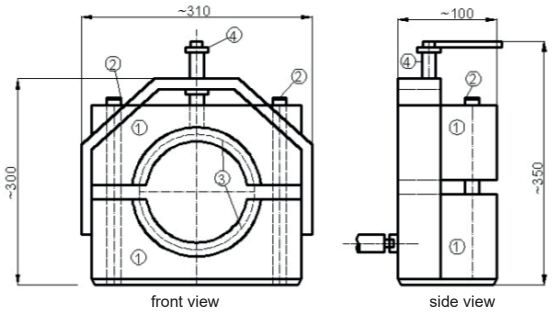

Fig. 2. Diagram of the Leutner apparatus [15]

The sample shearing is performed at a piston travel speed of 50 mm/min ±3 mm/min until the maximum force and shear moment on the core is obtained, the core is cut into two pieces or the maximum shear displacement (8 mm) limited by design considerations is reaches. During the test, the force-displacement relationship should be plotted.

2.1.4. The test using computed tomography scan

Computed tomography scanning is a non-destructive technique used to analyse the internal structure of materials using the X-radiation properties. One of the properties is the ability to penetrate matter, losing energy on its way according to Beer's law. The mentioned linear attenuation factor μ depends on the density of the tested material at each point through which the radiation beam passes. The creation of a tomographic image is based on the measurement of radiation absorption of the object. Performing a scan with the use of the tomograph is based on directing a beam of X-radiation to the object, and then recording the intensity of its absorption by a detector located on the other side of the object. The tomography scanner operating principle diagram is presented in the Figure 3.

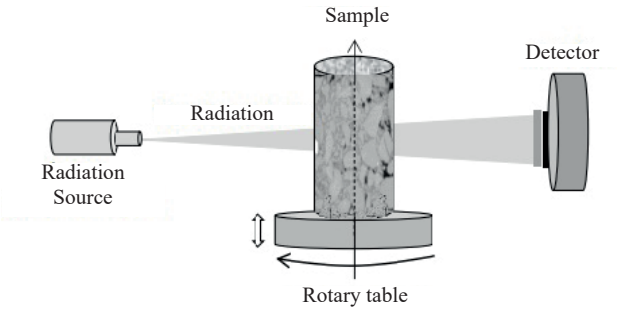

Fig. 3. Tomography scanner operating principle diagram [16]

Scanning is performed by irradiating the object with X-radiation while rotating the sample by 360° in relation to the stationary lamp and detector. The accuracy of the final mapping depends on the number of projections made during the rotation of the object. Once the projection images for multiple sections of the object are obtained, the image of the entire sample is reconstructed using the Radon transform. The final result is a three-dimensional grayscale image in which each shade of grey corresponds to a specific object density value. Lighter shades represent higher densities, while darker shades represent lower density materials.

The tests were performed with the use of a Nikon XT H 225 ST tomography scanner. A rotary lamp generating a radiation beam with a maximum voltage of 225 kV and a power of 450 W was used. The scans were performed with a voltage of 220 kV and a current intensity of 668 µA, using a 2 mm thick copper filter. These values were selected experimentally by scanning the sample several times to ensure the best possible parameters for a given type of material. After the compilation of almost 4.500, a three-dimensional model of the object was created with a resolution of approx. 84 µm for each of the samples. It was obtained by reconstructing the data and their initial processing – determining the axis of

rotation, noise reduction, sharpening the edges and applying filters in the CT Pro 3D program. Then the 3D model was analysed in the VG Studio Max 3.4 program.

3. COHESION CONTACT MODEL PARAMETERS IDENTIFICATION

The object of the research was the actual samples from the test boreholes consisting of the following layers: AC16W and RCM-FB with a diameter of 98 mm. One of the methods used to model the connections between the separate sections of the numerical model is the use of cohesive elements. Modelling the interlayer joint with "cohesive" type elements requires the definition of the material properties that enable the failure mechanism to be described. These elements can be used according to the material "traction-separation" law. The traction-separation law, used in the cohesion zone model, can be regarded as a phenomenological characteristic of the zone in which the separation will occur along the inter-phase zone. In addition, there are many models of the traction-separation failure criterion that were described in the works [13, 17].

A mechanism was used for the calculations, the characteristics of which include the description of initiation and evolution of failure until the total stiffness is lost. The basic constitutive law describing the "cohesive" type elements is the traction-separation failure criterion (breaking force – separation limit value) in which both standard direction (bursting) actions and effects related to failure due to tangential actions are taken into account [18] (Fig. 4).

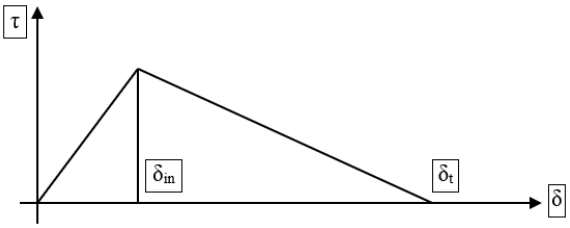

Fig. 4. The traction-separation failure criterion: τ – shear stress, δ – displacement, δ_{in} – displacement of finite element nodes corresponding to the moment of the failure initiation, δ_t – the value of the effective separation corresponding to the total loss of stiffness of the finite element

According to this model, it is possible to predict the failure of the zero thickness cohesive layer, and until the failure occurs it is assumed that the cohesive layer is working resiliently. The case of "Uncoupled traction-separation behaviour" was taken for the analysis, in which only the stiffness values located the main diagonal of the K matrix are taken into consideration, following the equation (1):

$$\tau = K \cdot \delta \tag{1}$$

where: τ – stress vector, K – diagonal stiffness matrix, δ – displacement vector.

The parameters of the cohesion contact model were obtained on the basis of the tests with the use of the Leutner apparatus. Identification of the parameters of the cohesion contact model was performed using one of the tests whose course was closest to the average value in the series of tests. Unfortunately, the available software does not have the feature to generate a digital file with the data. Nevertheless, the results of the course of the cohesive failure require mathematical formalisation. Therefore, the results obtained using the Leutner apparatus were interpolated from the photograph recording the course of the measurement using a unique calibration method with the use of graphic files [19]. The results obtained during the test using the Leutner apparatus are shown in Figure 5a.

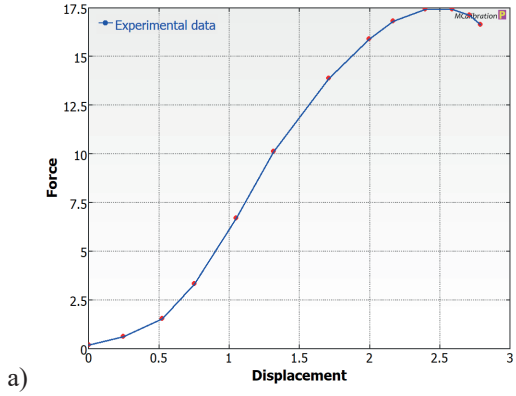

a)

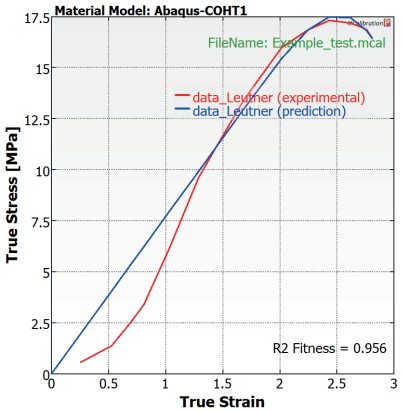

b)

Fig. 5. Identification of the cohesion contact model parameters: a) mapping the course of the graphic file examination; b) calibration of the cohesion contact model based on the Leutner test

Table 1. Cohesion contact model parameters (calculated based on Figure 5b)

***K*, MPa (interface shear stiffness)**	***S*, MPa (nominal shear stress)**	**Cohesive bond degradation value, –**	**Horizontal displacement, mm**
$K_{nn} = K_{ss} = K_{tt} = 7.66$	$S_{nn} = S_{ss} = S_{tt} = 3.15$	0	0
		0.000334188680278	0.88718327685
		0.000441358969059	0.967836302018
		…	…
		0.908219454635	2.98416193122
		0.967688817258	3.06481495639
		1	3.14546798156

The results are presented in Figure 5a were subjected to further analysis to identify the parameters of the cohesion contact model, including the stiffness values contained in the matrix *K* (1) and the nominal shear stress *S*. The linear criterion of the maximum stress ratio was adopted as the failure criterion [3]. For the full identification of the cohesion contact model parameters and their transfer in the form of a script, using the "spline" type interpolation function was required (Fig. 5b). As a result of the process of adjusting the interpolation-type function to the results of the experiment, the parameters of the cohesion contact model were obtained at the coefficient of determination at the level of $R^2 = 0.956$ – the parameters are given in Table 1.

Obtaining a description of the contact between the cohesive layers in such a compact form required supplementing the numerical model with contact properties using friction. Friction always occurs even, if the asphalt layers are not sprinkled with the asphalt emulsion. This is mainly due to the micro- and macrotexture of the grains and their wedging during the compaction of the asphalt mix [3]. The friction value depends on the normal stress applied. Based on the reference literature, the Coulomb friction model was utilised in the form of the friction coefficient $\varphi = 0.7$ [13]. The friction model was introduced into the cohesion contact model similarly as described in the work by Romanosha [4].

4. NUMERICAL MODEL

The numerical model was created based on a computed tomography photograph taken in sections of two samples. The first concerned the binding layer (code designation: MMA) while the second concerned the base course made of recycled material (code designation: RCM-FB). The numerical model was to simulate the course of the displacement between the real AC16W sample with a diameter of 98 mm and an additional sample of the RCM-FB layer with a diameter of 150 mm. Both layers of the road surface were subjected to the process of decomposition in various material phases. To simplify the process of splitting, the image was transformed into a binary file that divides the mix into mastic and aggregate phases [20] regardless of the type of the layer. Taking into account that the aggregate has at least 100 greater elasticity coefficient, the impact of aggregate differentiation was of secondary importance.

Based on computed tomography scans (Fig. 6a) batch files for the Abaqus program were generated. The separation of phases located in individual layers was obtained thanks to the script developed in the MatLab program. The aforementioned script defined the topology of mes mesh objects with the assumption of a plane stress distribution. As a result of the image processing, a file devided into sections differing in physical properties was obtained (Fig. 6b).

a)

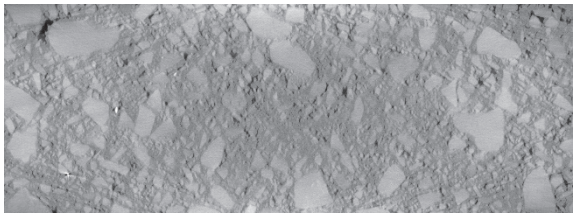

b)

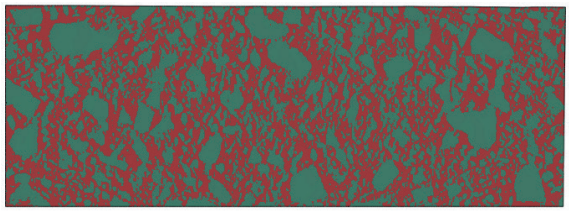

Fig. 6. Processing of the computed tomography image: a) actual grayscale image; b) image processes into sections of a different material

The materials were divided into two sections in each of the structure layers. The first one was assigned to the

aggregate and the second to the mastic. The material of each section was described using a linear elastic model. Since the stiffness of the aggregate was many times greater than the mastic, the same modulus of aggregate elasticity was assumed in both layers of the pavement to simplify the calculations. On the other hand, the mastic modulus of elasticity (in the MMA and RCM-FB layers) was determined experimentally by adjusting its value to the vertical displacement of cylindrical samples recorded in the DTC-CY test, according to EN 12697-26, Annex D [21]. The target value of the modulus of elasticity was determined numerically with the "golden ratio" gradientless method [22]. As a result, the physical parameters of the elastic model are presented in Table 2.

Table 2. Material data in the analysed layers

Material section	Modulus of elasticity [MPa]	Poisson Coefficient
Aggregate	10000 [23]	0.22
Mastic MMA	8	0.3
Mastic RCM-FB	6	0.3

The contact phenomenon was defined utilizing surface contact elements with zero thickness [24]. To describe the aggregate and mastic phase, two-dimensional elements using the plane state of stress CPS3 (3-node linear plane stress triangle) were used. Boundary conditions are defined at the bottom and left edge of the RCM-FB mix. Whereas to the upper surface of the MMA layer, a constant displacement of 0.5 mm directed downwards was applied. This procedure was aimed at mapping the displacement, which is considered in the Polish Catalogue as a value at which the pavement does not require strengthening [25]. The numerical model with boundary conditions is presented in Figure 7.

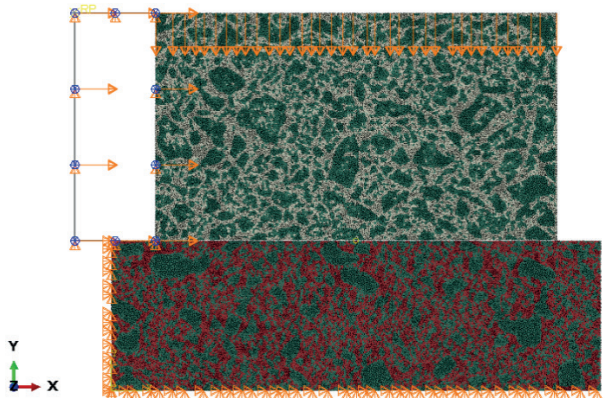

Fig. 7. Numerical model with boundary conditions

In the model, the upper MMA layer was displaced with the help of a perfectly rigid body element located at the left edge of the MMA layer. The level displacement (travel) introduced was 4 mm.

5. DEFORMATION STATE ANALYSIS

Maps of the main tensile (maximum) strains were determined in the first place. As a result, it was possible to quickly obtain information on areas where the bond between the aggregate and the mastic would potentially be lost. The map of the maximum main deformations (LE, MAX) is shown in Figure 8.

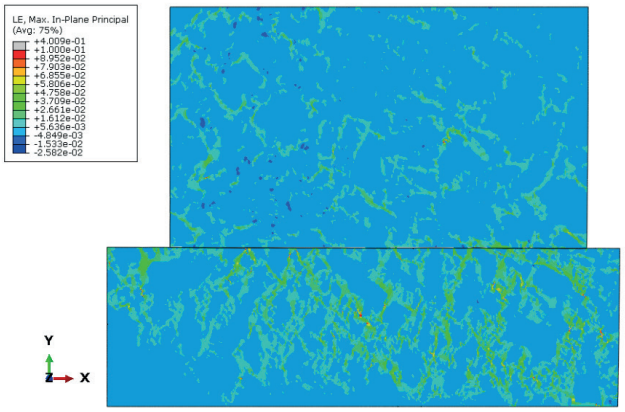

Fig. 8. Map of main logarithmic deformations (maximum)

It should be noted that the extreme level of main deformations occurred in the mastic in the RCM-FB layer, which had the lowest value of the modulus of elasticity. The deformation value was $\varepsilon > 4.78e^{-2}$ m/m, especially in the contact zone. Thus, such a level of interlayer displacement, indicating a loss of interlayer adhesion, will also initiate cracks in the RCM-FB layer. As a result, there is not only a risk of losing cohesion between the layers, but the aggregate detachment in the RCM-FB layer is also highly probable. It should be noted that the value of the main deformation is greater than the value of $\varepsilon = 1.0e^{-4}$ m/m, which means that the mastic deforms within the range of non-linear viscoelasticity. This is the extent to which the level of stress affects the material deformation characteristics. Thus, one should expect the accumulation of permanent deformations in the successive load cycles. This analysis was supplemented by a detailed assessment of the horizontal deformations in the RCM-FB layer (Fig. 9).

Due to the high stiffness of the aggregate in the RCM-FB layer (Fig. 9a) its deformation was small and probably will not initiate cracks in the grains. It should be noted that the extreme value of the horizontal deformation in the RCM-FB layer accumulated in the

a)

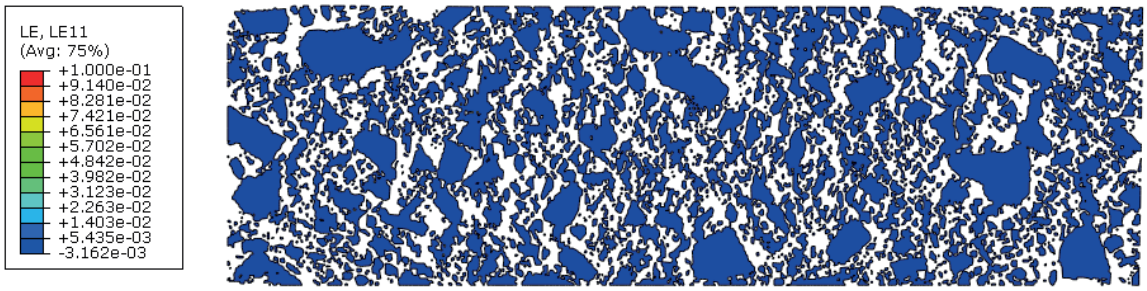

b)

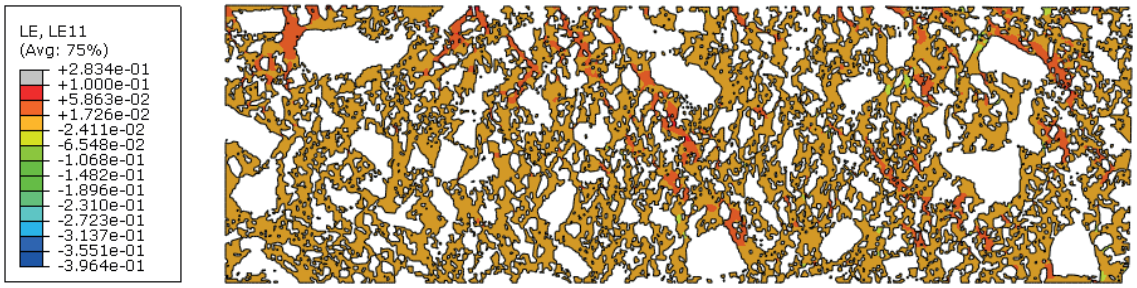

Fig. 9. Distribution of horizontal deformations LE11: a) in the aggregate section of the RCM-FB mix; b) in the mastic section of the RCM-FB mix

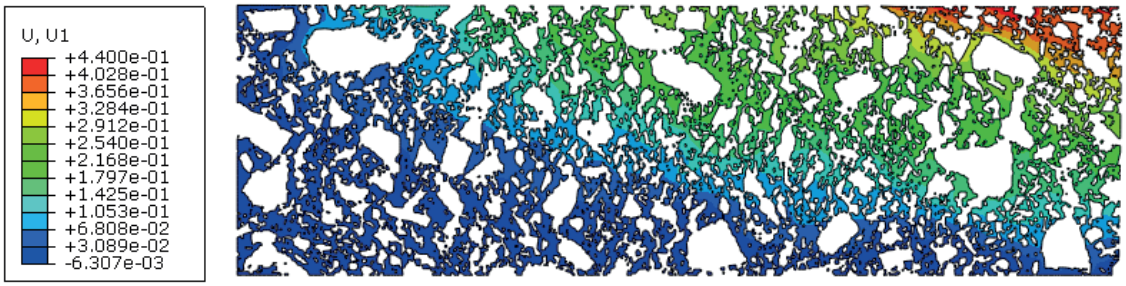

Fig. 10. Horizontal displacements (U1) in the mastic of the RCM-FB layer

contact zone (Fig. 9b). As a result, after exceeding the limit value of the displacement in the cohesion contact model (based on the Leutner test), large horizontal deformations will occur. The value of the deformation $\varepsilon > 1.776e^{-2}$ m/m will definitely cause a noticeable scratch on the RCM-FB mix surface [26] and the presence of unbound aggregate grains. It should be noted that such a large deformation cannot be transferred by the mastic in the RCM-FB layer. As a result, the loss of inter-layer adhesion caused by a large displacement between the layers in the areas of highly loaded intersections (e.g. roundabouts) will also manifest itself in large deformations of the base course and along with its degradation.

The presented pavement structure loading scenario is very similar to the scenario in which the vehicle wheel loads the pavement at its outer edge. Then, the lack of lateral resistance means that a large horizontal displacement may occur in the side edge of the underlayer, e.g. in the base course. At a certain value, damage known as edge cracks develop. The map of horizontal displacements (U1) in the RCM-FB layer mastic is presented in Figure 10.

As a result of the displacement of the MMA layer due to the high load in the RCM-FB layer mastic, a 0.44 mm displacement along the edge occurred. This is the type of displacement that will surely cause the edges of the base course to break off. Scratches in the RCM-FB layer will expedite the water penetration, which in low-temperature conditions will intensify further degradation of the layer system. Lack of proper connection between the RCM-FB and MMA layers caused by scratching of the base course edge area will cause further edge cracks, but this time in the MMA layer.

The analysis was supplemented by the estimation of the shear stresses caused by the delamination force in the contact zone between the MMA and MACA

layers. The results of the calculations are presented in Figure 11.

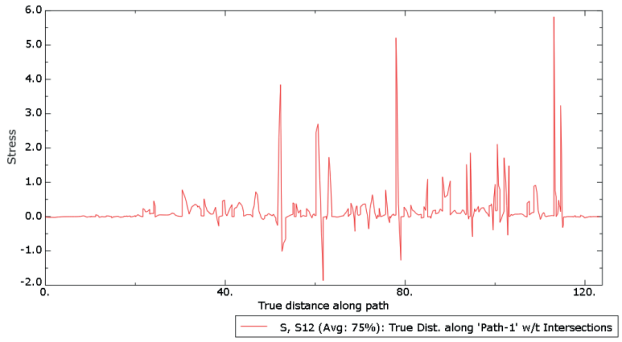

Fig. 11. The shear stress distribution in the contact zone (S12) along the length of the RCM-FB layer sample

It should be noted that, according to the Polish requirements, [15] the maximum shear stress between the bonding layer and the substructure that does not result in loss of interlayer adhesion, should be <0.7 MPa. No pressure force is applied by the Leutner apparatus, so the friction effect between the grains is of less importance. During the Leutner test, friction is caused mainly by wedging of the aggregate obtained during the compaction of the binding layer on the base course. Nevertheless, the analysis presented in the numerical simulation is a reliable representation of this state, where the wedging effect was initiated by the applied vertical deformation (U = 0.5 mm). When observing the course of the shear stress in the contact zone of the layers, it should be noted that there are several local areas where the shear stress exceeded 0.7 MPa. Shear stress > higher than 2.0 MPa was developed in at least 5 points. It indicates a very high value of the delamination force, which will negatively affect the further degradation of the connection. The singular areas where such high shear stress occurred were located in the aggregate-aggregate points of contact between the layers and where their overlapping occurred. It should be noted that the test with the use of Leutner apparatus allows obtaining the averaged value of stress between the layers. The shear stress reached the value of 0.7 MPa in many areas. Therefore, it confirms the correctness of the criteria adopted in Polish regulations for the biding layer-base course systems.

6. CONCLUSIONS

Based on the research and analyses performed, the following conclusions were formulated:

- Leutner test allows for satisfactorily quick identification of the cohesion contact model parameters;
- the use of structural analysis performed through computed tomography scanning allows for obtaining additional information on the phenomena that take place in the structure of aggregate-asphalt composites in road building, helpful in explaining the causes of roads degradation;
- loss of cohesion between the layers due to large horizontal deformation occurs in interaction with high tensile stress in mastic > $1.0e^{-4}$ m/m. As a result, the likely degradation of the aggregate-mastic bond will occur and the formation of numerous cracks in the base course constructed from recycled material;
- the numerical analysis is consistent with the Polish criteria for interlayer adhesion value at which the loss of the interlayer connection is likely to occur.

REFERENCES

[1] *Katalog typowych konstrukcji nawierzchni podatnych i półsztywnych* 2014.
[2] Obara P., Gilewski W.: *Dynamic Stability of Moderately Thick Beams and Frames with the Use of Harmonic Balance and Perturbation Methods*. Bulletin of the Polish Academy of Sciences Technical Sciences 2016, 64, doi:10.1515/bpasts-2016-0083.
[3] Judycki J., Jaskula P.: *Modelowanie teoretyczne wpływu sczepności międzywarstwowej na zachowanie się nawierzchni asfaltowych*, Generalna Dyrekcja Dróg Krajowych i Autostrad, Politechnika Gdańska, 2013.
[4] Romanoschi S.A., Metcalf J.B.: *Effects of Interface Condition and Horizontal Wheel Loads on the Life of Flexible Pavement Structures*, Transportation Research Record 2001, 1778, 123-131, doi:10.3141/1778-15.
[5] *Modeling of Asphalt Concrete*, Kim, Y.R. (ed.) McGraw-Hill Construction, ASCE Press; McGraw-Hill: Reston, VA : New York, 2009; ISBN 0-07-146462-X.
[6] Mazurek G.: *Liniowa i nieliniowa lepkosprężysta charakterystyka mastyksu asfaltowego w zakresie wysokich temperatur eksploatacyjnych nawierzchni*, Wydawnictwo Politechniki Świętokrzyskiej: Kielce 2019, ISBN 978-83-65719-60-7.
[7] Woldekidan M.F.: *Response Modelling of Bitumen, Bituminous Mastic and Mortar*, Technische Universiteit Delft, 2011.
[8] Owsiak Z., Czapik, P., Zapała-Sławeta J.: *Properties of a Three-Component Mineral Road Binder for Deep-Cold Recycling Technology,* Materials 2020, 13, 3585, doi:10.3390/ma13163585.

[9] Report TECHMATSTRATEG 1/349326/9/NCBR/2017 *The Innovative Technology Used the Binding Agent Optimization That Provides the Long Service Life of the Recycled Base Course*; National Centre for Research and Development (NCBR), 2018.
[10] Mazurek G., Buczyński P., Iwański M., Podsiadło M.: *Thermal Analysis-Based Field Validation of the Deformation of a Recycled Base Course Made with Innovative Road Binder*. Materials 2021, 14, 5925, doi:10.3390/ma14205925.
[11] Wirtgen Group *Cold Recycling Technology*, first edition, Wirtgen GmbH: Windhagen, 2012.
[12] Iwański M., Mazurek G., Buczyński P.: *Bitumen Foaming Optimisation Process on the Basis of Rheological Properties.* Materials 2018, 11, 1854, doi:10.3390/ma11101854.
[13] Jaskula P.: *Szczepność warstw asfaltowych w wielowarstwowych układach nawierzchni drogowych*; Wydawnictwo Politechniki Gdańskiej, Gdańsk, 2018; ISBN 978-83-7348-744-4.
[14] WT-1 Kruszywa do mieszanek mineralno-asfaltowych i powierzchniowych utrwaleń na drogach krajowych 2014.
[15] Jaskula P.: *Instrukcja laboratoryjnego badania szczepności międzywarstwowej warstw asfaltowych wg metody leutnera i wymagania techniczne szczepności,* 2014.
[16] Zelelew H.M., Almuntashri A., Agaian S., Papagiannakis A.T.: *An Improved Image Processing Technique for Asphalt Concrete X-Ray CT Images,* Road Materials and Pavement Design 2013, 14, 341-359, doi:10.1080/14680629.2013.794370.
[17] Zadpoor A.A., Sinke J., Benedictus R.: *The Mechanical Behavior of Adhesively Bonded Tailor-Made Blanks.* International Journal of Adhesion and Adhesives 2009, 29, 558-571, doi:10.1016/j.ijadhadh.2009.01.003.
[18] Campilho R.D.S.G., de Moura M.F.S.F., Ramantani D.A., Morais J.J.L., Domingues J.J.M.S.: *Tensile Behaviour of Three-Dimensional Carbon-Epoxy Adhesively Bonded Single- and Double-Strap Repairs,* International Journal of Adhesion and Adhesives 2009, 29, 678-686, doi:10.1016/j.ijadhadh.2009.02.004.
[19] Veryst *MCalibration Software from Veryst Engineering*; 47 Kearney Road, Needham, MA, USA, 2020;
[20] Gajewski M.: *Badania lepiszczy asfaltowych w reometrze dynamicznego ścinania – relacje konstytutywne lepkosprężystości, hipersprężystości i lepkohipersprężystości: Testing of bituminous binders in dynamic shear rheometer – constitutive relationships for visco-elasticity, hyperelasticity and visco-hyperelasticity*; Prace Naukowe, Politechnika Warszawska Budownictwo, Oficyna Wydawnicza Politechniki Warszawskiej, Warszawa 2018, ISBN 978-83-7814-768-8.
[21] EN 12697-26 D Bituminous Mixtures – Test Methods – Part 26: Stiffness.
[22] Kusiak J., Danielewska-Tułecka A., Oprocha P.: *Optymalizacja: wybrane metody z przykładami zastosowań*. Wydawnictwo Naukowe PWN, Warszawa 2009, ISBN 978-83-01-15961-0.
[23] Yazdani M., Sharifzadeh M., Kamrani K., Ghorbani M.: *Displacement-Based Numerical Back Analysis for Estimation of Rock Mass Parameters in Siah Bisheh Powerhouse Cavern Using Continuum and Discontinuum Approach.* Tunnelling and Underground Space Technology 2012, 28, 41-48, doi:10.1016/j.tust.2011.09.002.
[24] Smith M.: *ABAQUS/Standard User's Manual, Version 6.9*, Providence, RI: Simulia 2009.
[25] *Katalog typowych konstrukcji nawierzchni podatnych i półsztywnych* (Catalogue of typical flexible and semi-rigid pavements) (in polish) GDDKiA, Warszawa 2014.
[26] Alvarez A.E., Walubita L.F.. Sanchez F.: *Using Fracture Energy to Characterize the Hot Mix Asphalt Cracking Resistance Based on the Direct- Tensile Test,* Revista Facultad de IngenierÃ\-a Universidad de Antioquia, 2012, 126-137.